15th IAPR International Conference on Machine Vision Applications (MVA)
Nagoya University, Nagoya, Japan, May 8-12, 2017.

Robust Registration of Serial Cell Microscopic Images Using 3D Hilbert Scan Search

Yongwen Lai, Sei-ichiro Kamata
Graduate School of IPS, Waseda University
Japan
laiyongwen1991@fuji.waseda.jp

Zhizhong Fu
UESTC
China
fuzz@uestc.edu.cn

Abstract

Microscopic images are quite helpful for us to observe the details of cells because of its high resolution. Furthermore it can benefit biologists and doctors to view the cell structure from any aspect by using a serial images to generate 3D cell structure. However each cell slice is placed at the microscopy respectively, which will bring in the arbitrary rotation and translation among the serial slices. What's more, the sectioning process will destroy the cell structure such as tearing or warping. Therefore we must register the serial slices before rendering the volume data in 3D. In this paper we propose a robust registration algorithm based on an improved 3D Hilbert scan search. Besides we put forward a simple but effective method to remove false matching in consecutive images. Finally we correct the local deformation based on optical-flow theory and adopt multi-resolution method. Our algorithm is tested on a serial microscopy kidney cell images, and the experimental results show how accurate and robust of our method is.

1 Introduction

Regarding this topic, many researchers have been providing their contributions. The frequently used methods can be divided into two categories: rigid registration and non-rigid registration. The former method only helps in correcting the orientation and translation of the serial slices while the latter one not merely corrects the global transformation but also local deformation. In 2001, Alexis Roche[1] pointed out using block matching to extract the corresponding patch and minimize the summation of the distance between the central points of those patches. However, the block matching always brings in errors in microscopic cell images. In 2006, Pavel Koshevoy[2] proposed to extract SIFT feature and use RANSAC to estimate the transformation parameters. In 2006, Mosaliganti [3] proposed to use PCA alignment to rectify the orientation, and then adopted the maximization of mutual information to to obtain the optimal rigid transformation parameters based on a two-stage optimizer. Arganda-Carreras[4] proposed to use multiple algorithms to register the serial images. Firstly, correct the rigid transformation by minimizing MSE. Then extract the contour and grouped them to refine the rigid transformation parameters. Last, correct the local distortion by phase correlation method. However, this method is complex and time-consuming. Recently Ching-Wei Wang[5] proposed a coarse-to-fine method to align serial microscopic images. The author firstly correct the rigid transformation by minimizing the distance summation of corresponding SIFT points. And then the displacement field is refined by the bi-directional elastic B-spline model[6]. However, we tested this algorithm can not work well on kidney cell. There are many popular and conventional methods as well, such as maximizing mutual information or mean-square error based on gradient descent optimizer or conjugate descent optimizer, but the optimizers result in local optima to some degrees.

This paper is organized as follows. At first, we propose our overall framework in section 2. Then false matching removal method and 3D Hilbert scan search are presented in section 3 and 4. Section 5 is about experimental results.

2 Overview of our method

The overall framework of our proposed scheme is illustrated in Figure 1. In the rigid global registration stage, we apply 3D Hilbert scan to correct the rotation and translation of two consecutive image pairs. Firstly we extract the spectral-SIFT feature points[7](can be treated as landmarks) and match feature points in two images. Then the false matching feature points will be eliminated by our proposed method. In the next step, we align the matching feature points to obtain an estimated transformation parameters. Then we construct the 3D transformation parameters space around the estimated transformation parameters. Subsequently we maximize the mutual information to obtain the transformation parameters by 3D Hilbert scan search. In the local non-rigid stage, we correct the local deformation based on optical-flow theory[10].

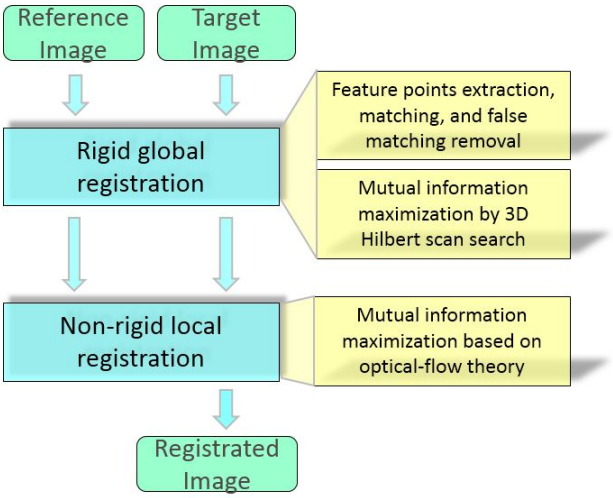

Figure 1. Registration framework to register two consecutive image pairs

Assume (x_r, y_r) denotes the coordinate of one pixel in the reference image I_r, while (x_t, y_t) is the coordinate of the corresponding pixel in target image I_t. The global rigid transformation of consecutive image pairs can be modeled by using three parameters (rotation angle θ, horizontal translation Δx, and vertical translation Δy). Hence the global rigid registration model can be written as

$$\begin{pmatrix} x_r \\ y_r \\ 1 \end{pmatrix} = \begin{pmatrix} cos\theta & -sin\theta & \Delta x \\ sin\theta & cos\theta & \Delta y \\ 0 & 0 & 1 \end{pmatrix} \begin{pmatrix} x_t \\ y_t \\ 1 \end{pmatrix} \quad (1)$$

Therefore, The global rigid registration can be represented as multi-parameter optimization problem. We adopt and modify 3D Hilbert scan search and this will be explained in section 4.

3 False matching removal

As mentioned in overview, correct matching feature points are necessary prior the 3D Hilbert scan. Lowe[9] suggested to eliminate false matching feature points based on the ratio of Euclidean distance from the query descriptor to its closest match and second closest match in descriptor space. However some error matches are still reminded. The other frequently used method is RANSAC. Randomly selecting several matching feature points to compute the transformation matrix for several times. The obtained transformation matrix will be able to satisfy most matching feature points. Then the leftover points are false matching feature points. Nevertheless, this method is time consuming.

In our method, we adopt spectral-SIFT points[7]. It is because spectral-SIFT is based on continuous scale space, it can obtain more keypoints compared with discrete scale space. The extracted Spectral-SIFT feature points are shown in Figure 2(b) compared with SIFT feature points shown in Figure 2(a). The number of feature points in (a) is more than (b).

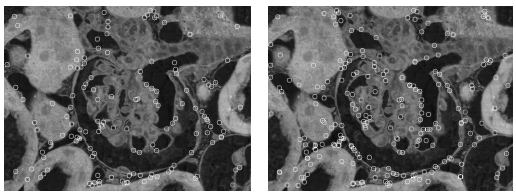

(a) (b)

Figure 2. (a) SIFT feature points. (b) Spectral-SIFT feature points.

At every keypoint, 128-Dimension feature descriptor is computed. Keypoints in two images can be matched to each other based on descriptors. We assume the consecutive image only suffered from minor change in global scale, so that the false matched feature points can be deleted by the ratio defined in equation 2. Let feature points set of reference image and target image are $\{p_1, p_2, .., p_n\}$ and $\{q_1, q_2, .., q_n\}$ respectively. p_i and q_i are matching feature points. We eliminate those false matching pairs by calculating the ratio of the distances between two matching pairs as follow

$$ratio = \frac{distance(p_i, p_j)}{distance(q_i, q_j)} \quad (2)$$

Table 1. False matching removal comparison between proposed method and RANSAC. False and true mean average number of false matching and true matching respectively.

Method	False	True	Time(s)
Proposed method	1.2	217.5	0.125
RANSAC	3.7	150.8	0.420

Table 2. Experimental result about estimated transformation parameters. Here FMR means false match removal.

Method	Horizontal	Vertical	Rotation	Accuracy
With FMR	2.0	5.0	0.0	0.7980
Without FMR	0.0	5.0	0.0	0.7820

In our experiment, if the ratio is less than 0.8 or larger than 1.2, it can be assigned as false matched pair. After removing the false matching, the correct matching is shown in Figure 3.

Figure 3. Matched feature points

Here, a table of experimental comparisons about false matching removal is shown in Table1.

Here, we also attach a middle experimental result in Table2 about estimated transformation parameters when we process a pair of two consecutive images.

4 3D Hilbert scan search

Hilbert scan is a scanning method guided by N-Dimension Hilbert space filling curve. Here, horizontal translation Δx, vertical translation Δy and rotation angle θ are three axises in this 3D space. After performing Hilbert scan, the 3D space reduces to 1D space as shown in Figure 4. The main steps of optimal transformation parameters searching based on 3D Hilbert scan as follow,

Step 1 Construct the 3D transformation parameter space(Δx, Δy, θ).

Step 2 Sample the parameter space into discrete points.

Step 3 Use 3D Hilbert scan to reduce the 3D space to 1D space.

Step 4 Find the optimal transformation parameters in the search space using mutual information as the similarity measurement.

At step 1, we first obtain the coarse estimated rigid transformation parameters(Δx_e,Δy_e,θ_e) by computing

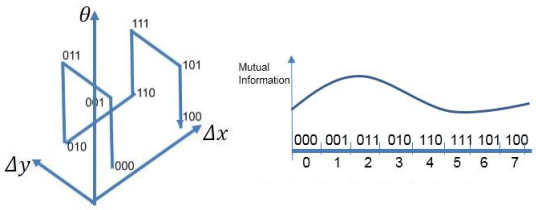

Figure 4. 3D transformation space and 3D Hilbert scan reduces 3D space to 1D space[8]

the following equation

$$(\Delta x_e, \Delta y_e, \theta_e) = arg \min_{(\Delta x, \Delta y, \theta)} \sum_{i=1}^{N} \|T(p_i) - q_i\|_2 \quad (3)$$

Here T means the rigid transformation matrix which consists θ, Δx, and Δy in equation (1). p_i and q_i are the coordinates of matching feature points. Then we construct a cube in the 3-D space with $[\Delta x_e - L/2 + 1, \Delta x_e + L/2]$, $[\Delta y_e - L/2 + 1, \Delta y_e + L/2]$, $[\theta_e - L/2 + 1, \theta_e + L/2]$ based on the estimated transformation parameters. The size of the search space is $L \times L \times L$ corresponding to the size of 3D Hilbert scan space. In our experiment, we assigned L as 10.

Step 2 and 3 are done as previously stated. At step 4, in the beginning, we equally divide the 1-D sequence into k parts using $k+1$ initial points with interval Δd. We denote the i-th candidate point as C_i in a candidate set. We describe the methodology by an example as shown in Figure 5. Here mutual information abbreviated as MI. For one candidate C_i, its left and right adjacent points are $C_i - \Delta d$ and $C_i + \Delta d$, and if $MI(C_i - \Delta d) < MI(C_i + \Delta d)$, then $M_i = (C_i + \Delta d/2)$. Next comparing M_i to C_i, if $MI(C_i) < MI(M_i)$, replace C_i with M_i, otherwise C_i is still in the candidate set. Then 70% number of candidates according to the MI amount remind in candidates set in our experiment.

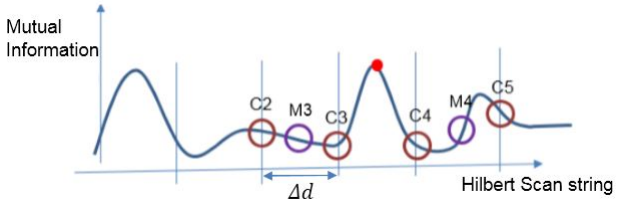

Figure 5. An example to update the candidate points to show how to obtain local optima. The red point is the global optima.

In Figure 5, you can notice that if we process by the conventional method, the result fails to get global optima presented as the red point. Therefore, we propose to randomly change the initial candidates by the equation (4) for several times. If the mutual information on new candidate is larger than current candidate, then we update the candidate to new location.

$$NL(i) = C \times Random(1) \times (OL(i) - CL(i)) + CL(i) \quad (4)$$

Here $NL(i)$ denotes new candidate, $CL(i)$ is current candidate, and $OL(i)$ is the optimal candidate point up to present iteration. $Random(1)$ is arbitrary number from 0 to 1. Finally, We correct the rigid transformation by 3D Hilbert scan search in this stage.

In the next stage, we rectify the local deformation which comes from the sectioning part(like tearing, warping) by the work from Tang, et al. [10].

$$v(x)\nabla(I_r(x)) = I_t(x) - I_r(x) \quad (5)$$

here $I_t(x)$ and $I_r(x)$ are the gray value of the I_t and I_r at the x location. $\nabla(I_r(x))$ is the gradient of the I_r at x. And $v(x)$ is the displacement from I_t to I_r at x. For global continuity, Gaussian filter $G_\sigma(x)$ is utilized to smooth the displacement field, so we modify the resulting deformation field by

$$v_{n+1}(x) = G_\sigma \otimes (v_n(x) + \frac{(I_t(x) - I_r(x))\nabla(I_r(x))}{k||\nabla(I_r(x))||^2 + \alpha(I_t(x) - I_r(x))^2}) \quad (6)$$

In this equation, it need k and α to allow large deformation in order to improve accuracy, and the algorithm should be more precise when the difference of MI change less than a threshold, so k and α need become larger. Here we propose a default α and adaptively change k by the following equation.

$$\text{k} = \begin{cases} k_0 & MI > \epsilon \\ k_1 - e^{\frac{-(n-n_0)}{b}} & MI\epsilon \end{cases}$$

Here ϵ is a preset threshold. n_0 is the iteration time when MI reach a present threshold β.

The displacement field can be updated $v_n(x)$ step by step. In every loop, the target image is deformed by the displacement field and the mutual information amount is computed. If the amount exceeds our preset threshold or process fulfills the iteration number, the process is forced to end. In this stage, we adopt the validation model[5] which can avoid displacement error propagation.

5 Experiment

5.1 Evaluation method

For evaluating our proposed method, we adopt the evaluation method proposed in paper[5]. The accuracy is computed as

$accuracy = \sum_{(x,y) \subset S} a(x,y)/M$,

where S is the common region of the adjacent image pairs. M is the number of pixels in the common region. $a(x,y)$ is defined as follows

$$a(x,y) = \begin{cases} 1 & |I_r(x,y) - I'_t(x,y)| < threshold \\ 0 & else \end{cases},$$

where I_r is the reference image while I'_t is the registered image. The threshold is set as 15 in our experiment. The reason for us to select 15 as threshold is to ease our comparison with the reference paper [5].

5.2 Material and experimental results

In this section, a serial microscopic Kidney cell images are employed to evaluate the performance of our proposed registration scheme. The number of the slices is 21 and the resolution of the image is 1208x928.

Table 3. The average accuracy comparison of different methods. Landmark indicates rigid transformation by aligning the landmarks. MMI is rigid transformation by maximizing MI by gradient descent optimizer.

Method	Landmark	MMI	Wang's	Ours
Accuracy	0.8450	0.8567	0.8475	0.8699
Time(s)	1.23	6.12	7.45	7.65

In figure 6, we demonstrate the overlap of two adjacent images. Figure 6(a) shows that there exist false aligned pixels between consecutive images. However in the Figure6(b) and Figure 6(c), the false aligned pixel are eliminated.

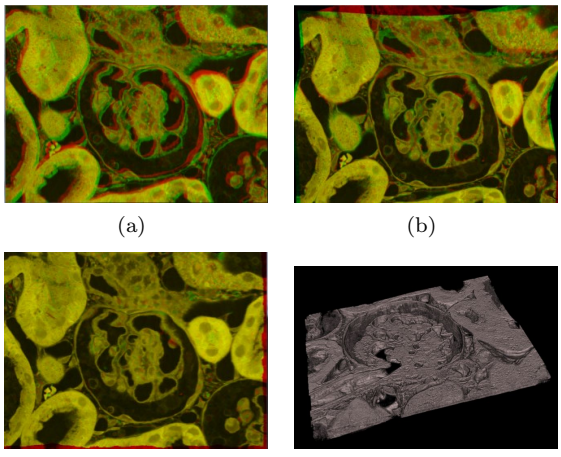

(a) (b) (c) (d)

Figure 6. (a) The overlap of original consecutive images. (b) The overlap of registered image by method[5]. (c) The overlap of registered image by proposed method. Yellow covered region shows that pixels registered correctly, while the green or red pixel region show that pixels are faultily registered.

We also test the average accuracy and they are shown in the table 3. We test the same data on Chingwei-Wang's code, and our method performs better than Chingwei-Wang's method[5] as well as other conventional methods. The average accuracy of our method is 86.99% while Chingwei-Wang's method is 84.75%. Besides that, we also show the robustness of our method by box-plot. Here is a short discussion between this paper and Wang's paper. Wang applied B-Spline method which computes the displacement vector on control points. Then displacement vectors on non-control points are interpolated from the displacement vector on control points based on B-Spline function. But in this paper, we use optical-flow method which computes displacement vector on every pixel directly.

Figure 7 shows the box-plot, the less the expansion of box, the more robust of the method. The box of our method shows the least expansion, in other words, it shows the highest robustness of our method is.

As for 3D visualization system, we eliminate image intensity difference due to difference in imaging condition. Then consecutive images are registered. Finally we can visualize the volume data based on ray-casting. Figure 6(d) shows the 3D Kidney cell structure.

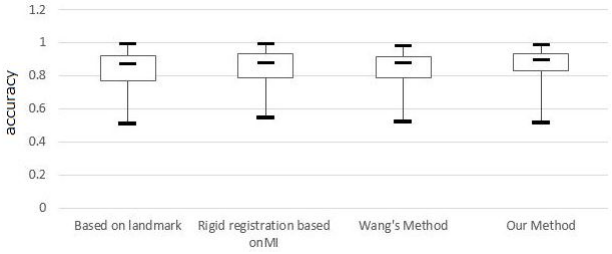

Figure 7. Robustness comparison

6 Conclusion

In this paper, we proposed a novel robust registration method to register serial microscopic cell images accurately. We successfully removes those false matching pairs by calculating the distance ratio in two consecutive images. And then global rigid transformation can be corrected by using 3D Hilbert scan search. Finally we rectify the local deformation. The experimental results show that our method performs better than other methods.

References

[1] S. Ourselin, A. Roche, et al, Reconstructing a 3d structure from serial histological sections. *Image and vision computing*, 19(1):pp: 25–31, 2001.

[2] P. Koshevoy, T. Tasdizen, et al, Assembly of large three-dimensional volumes from serial-section transmission electron microscopy. In *Proceedings of 2006 MICCAI Workshop on Microscopic Image Analysis with Applications in Biology*, pp: 1–8, 2006.

[3] K. Mosaliganti, T. Pan, et al. Registration and 3d visualization of large microscopy images. In *Medical imaging*, pp: 61442V–61442V. International Society for Optics and Photonics, 2006.

[4] I. Arganda-Carreras, R. Fernndez-Gonzlez, et al. 3d reconstruction of histological sections: Application to mammary gland tissue. *Microscopy research and technique*, 73(11): pp: 1019–1029, 2010.

[5] C.-W. Wang, E. B. Gosno, et al, Fully automatic and robust 3d registration of serial-section microscopic images. *Scientific reports*, 5, 15051, 2015.

[6] I. Arganda-Carreras, C.O.S. Sorzano, et al. Consistent and elastic registration of histological sections using vector-spline regularization. In *International Workshop on Computer Vision Approaches to Medical Image Analysis*, pp: 85–95. Springer, 2006.

[7] G. Koutaki and K. Uchimura. Scale-space processing using polynomial representations. In *Proceedings of the IEEE Conference on Computer Vision and Pattern Recognition*, pp: 2744–2751, 2014.

[8] T. Li and S. Kamata. A two-stage point pattern matching algorithm using ellipse fitting and dual hilbert scans. *IEICE transactions on information and systems*, 91(10): pp: 2477–2484, 2008.

[9] D. Lowe. Distinctive image features from scale-invariant keypoints. *International journal of computer vision*, 60(2): pp: 91–110, 2004.

[10] Zhenchao Tang, Peng Xue, et al, An effective Non-rigid Image Registration Method Based on Active Demons Algorithm. *2016 IEEE 29th International Symposium on. IEEE, 2016: pp: 124-129.*,